

Therapeutic Response Monitoring of anti-HER1 therapy with PET imaging biomarkers in Esophageal Squamous Cell Carcinoma Model

Yong Hwa Hwang, In Ho Jeong, Joo Hyun Kang, Yong Jin Lee, Kwang Il Kim, Tae Sup Lee
Brain Disease Imaging Research Team, RIRAMS, KIRAMS, Republic of Korea
nobelcow@kirams.re.kr

1. Introduction

Esophageal cancer is the eighth most common cancer worldwide and the sixth most common cause of death from cancer [1]. Two major histologic types of esophageal cancer have been defined: esophageal squamous cell carcinoma (ESCC) and esophageal adenocarcinoma. Most patients with esophageal cancer in Asia such as Japan and China have squamous cell carcinoma (SCC) [2]. There have been recent advances in surgical techniques, chemotherapy and radiotherapy, but outcome for patients with esophageal cancer remains poor. Therefore, novel therapeutical strategies such as molecular-targeted therapy, including small molecule inhibitors of tyrosine kinases (TKIs) and monoclonal antibodies (mAbs) are needed [3].

Epidermal growth factor receptor (EGFR, HER-1) overexpression is common in ESCC. Earlier immunohistochemical studies showed that 40-50% of ESCC tumors express EGFR which is associated with disease progression and prognosis. These results indicate that the signaling pathway involving EGFR may be related in biological roles of ESCC tumor and suggests that EGFR could be a proper molecular target. High levels of EGFR expression may be considered to be a pre-treatment predictor of anti-HER-1 therapeutic efficacy. Cetuximab, a human-mouse chimerized IgG₁ antibody with a high affinity for the EGFR, blocks the binding of ligand and induces the internalization and downregulation of EGFR. Anti-tumour activity of cetuximab has been reported in pre-clinical studies and clinical trials of esophageal cancer [4].

Imaging biomarker could be used for the screening of pertinent targets or patients and the monitoring therapeutic efficacy. *In vivo* imaging of immuno-positron emission tomography (Immuno-PET) might provide a valuable strategy for evaluating EGFR expression level in tumor and predicting tumor response to anti-EGFR targeted therapy. ⁶⁴Cu labeled cetuximab as an Immuno-PET imaging agent has been evaluated in several tumor-bearing mouse models. In molecular targeted therapy, noninvasive imaging biomarker could provide valuable informations for screening patient population and assessing early response to targeted therapy, thereby such information may improve therapeutic outcomes. We provide that both ⁶⁴Cu-labeled cetuximab and FDG as PET imaging biomarkers may be useful for monitoring patient response to cetuximab therapy.

2. Materials and Methods

2.1. cell cultures

ESCC cell lines, TE-4 and TE-8 were obtained from RIKEN Bioresource center (Japan) and grown in RPMI 1640 medium, and A431 and were purchased from ATCC (USA) and maintained in DMEM. All media were supplemented with 10% FBS and 1% antibiotics/antimycotics. Cultures were maintained at 37°C in humidified 95% air and 5% carbon dioxide atmosphere.

2.2. Flow cytometry

Cells were incubated with cetuximab or the isotype control antibody for 1 h at RT. After washing twice with PBS containing 1% BSA, the cells were incubated with FITC-conjugated anti-human IgG for 1 h at RT. Stained cells were analyzed for antibody binding using FACS Calibur (BD Immunocytometry System) and CellQuest software.

2.3. Preparation and characterization of ⁶⁴Cu-PCTA-Cetuximab

Cetuximab (Merck Serono, Switzerland) was buffer exchanged and concentrated to 10 mg/mL in 0.1 M sodium bicarbonate buffer using Vivaspinn ultracentrifugation tubes (Sartorius). A 10-fold molar excess of *p*-SCN-Bn-PCTA over antibody in DMSO was added to the antibody in 0.1 M sodium bicarbonate buffer. Conjugation was allowed to proceed at RT for 2 h. Unconjugated chelator was removed by dialysis.

⁶⁴Cu was produced at KIRAMS by 50 MeV cyclotron irradiation. ⁶⁴CuCl₂ was incubated with PCTA-conjugated cetuximab for 60 min at room temperature. Quality control was performed by instant thin layer chromatography-silica gel (ITLC-sg, Pall) with a mobile phase of 20 mM citrate buffer with EDTA.

2.4. Cell proliferation inhibition assay

TE-4 and TE-8 cells were plated in 6-well plate at 2.5×10^4 cells per well and incubated for 18 h. Cells were treated with various concentrations of cetuximab in RPMI-1640 medium with 2% FBS. After 5 day incubation, viable cells were counted in a cell counter (ADAM automated cell counter, Digital-Bio, South Korea).

2.5. Immunotherapy

When the tumor volume reached 100-200 mm³ (3~4 wks after inoculation), mice (n = 6 or 7/group) were intravenously administered with cetuximab or isotype (Rituximab) antibody (50 mg/kg) twice per week for 4 weeks. Tumor volume was calculated by long diameter x (short diameter)² / 2 and body weight were measured thrice a week.

2.6. Small animal PET imaging

PET imaging of tumor-bearing mice was done on a small animal PET scanner (microPET R4, Concorde, Knoxville, TN). ⁶⁴Cu-PCTA-cetuximab (3.7 MBq) was injected intravenously into the mice and static scans were acquired for 60 min at 2, 24, 48, and 72 h post-injection. Quantitative data were expressed as standardized uptake value (SUV), which are defined as the counts per second per pixel in a region of interest divided by total counts per second per pixel in the mouse. ¹⁸F-FDG (7.4 MBq) was injected intravenously 1 h prior to scan and static scans were obtained for 20 min. PET images were analyzed and quantified.

2.7. Immunohistochemistry

Following the third dose of isotype or cetuximab, the mice were sacrificed. The tumors tissues were excised, fixed in 4% paraformaldehyde, dehydrated and embedded in paraffin. Subsequently, Terminal deoxynucleotidyl transferase-mediated dUTP nick end labeling (TUNEL) and phosphorylated Akt (pAkt) staining were carried out on tumor sections. In random fields, the number of TUNEL-positive nuclei per field was determined. The pAkt staining index (SI) was defined as the percentage of positive nuclei within the total number of nuclei.

2.7. Statistical analysis

Quantitative data are represented as the mean ± SD and statistical analysis was performed by one-way ANOVA or Student's t test using GraphPad Prism 5. *P* values of < 0.05 were considered statistically significant.

3. Results and discussion

Flow cytometric analysis (Fig. 1A) showed similar result with western blot data. As determined by western blot and flow cytometry, TE-8 cell line expressed relatively high levels of EGFR and the other three cell lines showed intermediate EGFR expression.

To determine the cell-surface EGFR expression using ⁶⁴Cu-PCTA-cetuximab, cell binding assay was performed. Binding studies were performed in live cells at 4°C to inhibit internalization of radiolabeled cetuximab. A431, a human epidermoid carcinoma, and

U87MG, a human glioblastoma, were used as a positive and negative control in this study, respectively.

As shown in Figure 1B, it was found TE-8 cells (70.9±1.5%) have high EGFR expression in close to A431 cells (77.5±1.6%). TE-4 (15.2±0.3%) cells have relatively low EGFR expression. This result indicated that binding of ⁶⁴Cu-PCTA-cetuximab represents the number of EGFR molecules on the cells.

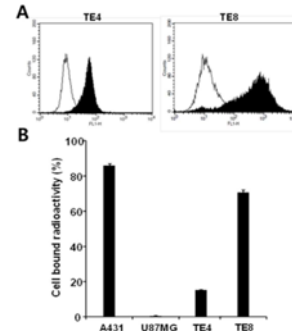


Fig. 1. Analysis of EGFR expression and cytotoxicity of cetuximab on ESCC cell line. A, Flow cytometry using cetuximab. B, Cell binding assay of ⁶⁴Cu-PCTA-cetuximab.

We examined the anti-proliferative effect of cetuximab against high EGFR expressing cell line, TE-8 cells and low EGFR expressing cell line, TE-4 cells. Cetuximab-induced cell growth inhibition was found in high EGFR expressing TE-8 cells, while it was minimal in low EGFR expressing TE-4 (Fig. 2).

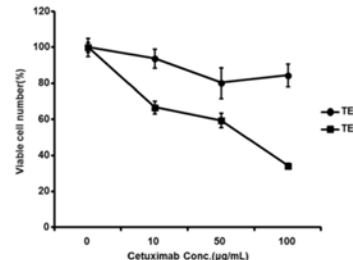


Fig. 2. Cytotoxicity of cetuximab on TE-4 and TE-8 cells for 5 days cetuximab treatment.

With 10 µg/mL cetuximab, TE-8 cells showed 57.2±3.9% viability compared with control, however, TE-4 cells still kept more 80% viability even with 100 µg/mL cetuximab.

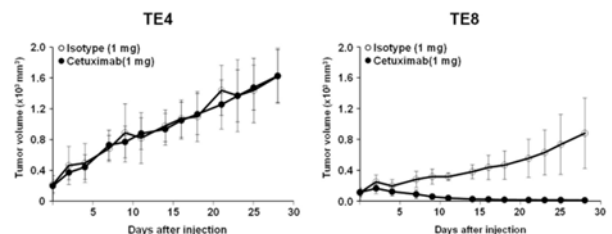


Fig. 3. Antitumor effect of cetuximab in ESCC tumor model. TE-4 and TE-8 tumor growth in ESCC xenograft model treated with isotype or cetuximab.

Anti-tumor effects of cetuximab were assessed in TE-4 and TE-8 xenograft models (Fig. 3). In isotype group,

the growth rate of TE-4 tumors was faster than that of TE-8 tumors. TE-8 tumor growth inhibited after second administration of cetuximab and TE-8 tumor markedly regressed by cetuximab treatment, but TE-8 tumor volume continuously increased in isotype treatment. TE-8 tumor volume in cetuximab treatment group showed a statistically significant difference from 14 days ($P < 0.01$). Cetuximab treatment was well tolerated in both TE-4 and TE-8 xenograft models, and no apparent body weight loss was observed.

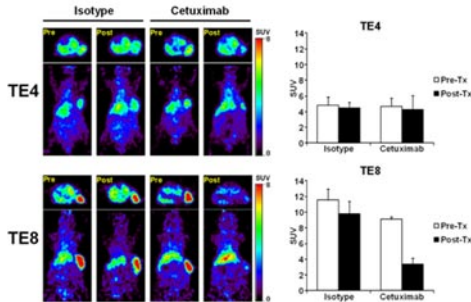


Fig. 4. Immuno-PET imaging of EGFR expression level in ESCC xenograft model before and after cetuximab treatment.

To assess tumor response to cetuximab therapy, immuno-PET (Fig. 4) and FDG-PET (Fig. 5) imaging were used. ^{64}Cu -PCTA-cetuximab immuno-PET images were obtained for each animal before treatment and after one week of treatment in TE-4 and TE-8 xenograft models. In TE-4 tumors, there was no statistically significant difference between SUV of pre-treated group and SUV of post-treated group in isotype treated or cetuximab treated mice (Fig. 4A and C). For TE-8 tumors, there was 65.9% statistically significant SUV reduction in cetuximab treated mice ($P < 0.01$). EGFR expression level of TE-8 tumors markedly reduced by cetuximab treatment. Although SUV of TE-8 tumors in isotype treated mice seemed to trend downward when comparing to SUV of pre-treated group, the trend was not significant.

FDG-PET imaging was also performed before and after one week treatment. Treatment with isotype or cetuximab did not significantly alter FDG uptakes in TE-4 tumor (Fig. 5).

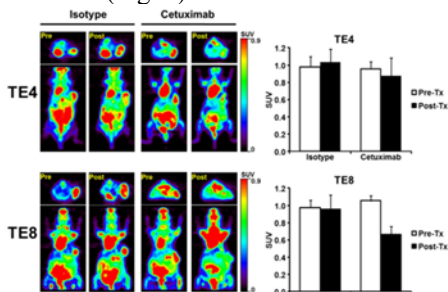


Fig. 5. Therapeutic response monitoring by cetuximab treatment using FDG-PET imaging in ESCC xenograft model before and after cetuximab treatment.

Cetuximab treatment significantly reduced FDG uptake in TE-8 xenograft model ($P < 0.05$). Isotype treatment had no effect on FDG uptake in TE-8 tumor.

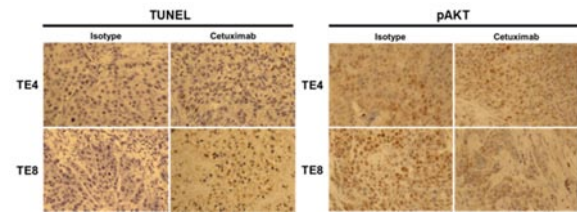


Fig. 6. Immunohistochemical staining of TUNEL and phospho-Akt of TE-4 and TE-8 tumors by isotype or cetuximab treatment.

TUNEL assay was performed to evaluate cell apoptosis induced by cetuximab treatment in TE-4 and TE-8 tumors. In both tumors, apoptosis was almost not observed after isotype treatment. TUNEL positive apoptotic cells were more visualized in TE-4 tumor by cetuximab treatment compared with isotype treated TE-4 tumor, but statistically insignificant. Apoptotic cells markedly increased in cetuximab treated TE-8 tumors compared with isotype ($P < 0.01$), indicating that cetuximab treatment increased apoptosis of high EGFR expressing TE-8 cells (Fig. 6). pAkt immunoreactivity was significantly reduced in TE-8 tumor by cetuximab treatment compared with isotype. In TE-4 tumors, pAkt positivity slightly increased by cetuximab treatment compared to isotype, however the difference was non-significant. pAkt staining suggested that cetuximab treatment inhibited the PI3K/Akt pathway on TE-8 tumor.

4. Conclusion

This study shows that ^{64}Cu -PCTA-cetuximab immuno-PET and FDG-PET could be used as potential pharmacodynamic PET imaging biomarkers of response to cetuximab treatment in ESCC tumors by anti-HER1 targeted therapy. ^{64}Cu -PCTA-cetuximab immuno-PET imaging biomarker may be useful for selecting patient that express target molecules and monitoring therapeutic efficacy of molecular targeted therapy in clinical trial.

REFERENCES

- [1] Ferlay J, Shin HR, Bray F, Forman D, Mathers C, Parkin DM. Estimates of worldwide burden of cancer in 2008: GLOBOCAN 2008. *Int J Cancer*, Vol. 127, No. 12, pp2893-2917, 2010.
- [2] Law S, Wong J. Current management of esophageal cancer. *J Gastrointest Surg.*, Vol. 9, No. 2, pp291-310, 2005.
- [3] Aklilu M, Ilson DH. Targeted agents and esophageal cancer--the next step? *Semin Radiat Oncol.*, Vol. 17, No. 1, pp62-69, 2007.
- [4] Kawaguchi Y, Kono K, Mimura K, et al. Targeting EGFR and HER-2 with cetuximab- and trastuzumab-mediated immunotherapy in oesophageal squamous cell carcinoma. *Br J Cancer*, Vol. 97, No. 4, pp494-501, 2007.